ISSN: 2178-7727
DOI: 10.17648/acta.scientiae.6369

DIELECTRIC RESONATOR ANTENNA DESIGN FOR MIMO-BASED WIRELESS COMMUNICATION SYSTEMS

Simran Taneja
Department of Electronics & Communication MMEC, MM (Deemed to be University) Mulana Ambala, India
simrantaneja6499@gmail.com

Dr. Tarun Gulati
Department of Electronics & Communication MMEC, MM (Deemed to be University) Mulana Ambala, India
gulati_tarun@mmumullana.org

Abstract

This work introduces a rack-shaped two-element dielectric resonator antenna (DRA) based multiple-input multiple-output (MIMO) system featuring improved axial ratio features for ultra-wideband (UWB) operations. The proposed antenna configuration employs two rectangular radiator elements modified into rack-shaped dielectric resonators to excite multiple resonant modes, namely HEM_{111}, HEM_{121}, and HEM_{212}, at 7.3 GHz, 9.3 GHz, and 10.74 GHz, respectively. The rack-based configuration markedly enhances the bandwidth effectiveness over the UWB wavelength spectrum. An inverted T-shaped magnetic strip is employed to attain elliptical polarisation while efficiently regulating both axial ratio spectrum & susceptibility spectrum, yielding a broad impedance spectrum of 101.87%. Simulated & measured outcomes demonstrate strong concordance and validate UWB functionality from 3.54 to 10.89 GHz. The MIMO effectiveness is assessed based on the envelope correlation ratio ($ECC \leq 0.0059$), broadness gain ($DG \geq 9.93$ dB), total reflection active coefficient (TARC) across various phases positions, grouping delay (ranging from 0.96 to −2.1 ns), and channel capability loss ($CCL \leq 0.4$ bits/s/Hz, excluding the 8.8–9.6 GHz band). The outcomes demonstrate that the suggested transmitter meets typical MIMO requirements and is appropriate for high-data-rate uses within the C- & X-band spectrum categories.

Keywords: MIMO, UWB, MIMO, RDRA

I. Introduction

Ultra-wideband (UWB) telecommunication has garnered considerable interest with the Federal Broadcasting Administration designating the 3.1–10.6 GHz unrestricted spectrum range for business utilisation. Ultra-Wideband (UWB) technologies possesses found widespread applications in wireless sensor networks, biomedical systems, and healthcare communication due to its low power spectral density, simple hardware architecture, high data transmission rates, low implementation cost, high ranging accuracy, and low power consumption [1]. However, the design of UWB antennas presents several challenges, including miniaturization, high radiation efficiency, stable gain performance, and mitigation of electromagnetic interference from coexisting narrowband systems. In the past few years, DRAs had become prominent contenders for UWB applications owing to their low conductor losses, highest radiation efficiency, design flexibility, and ease of excitation [2], [3]. To achieve compact antenna dimensions, high-permittivity dielectric resonators are preferred, as the physical size of a dielectric resonator is inversely proportional to its relative permittivity [4]. It has been reported that when the dielectric constant of the resonator is ≥ 9, radiation efficiencies of ≥ 75% could be achieved. Furthermore, stacked DR configurations have been employed to preserve antenna gain and radiation efficiency [5].

To accommodate increasing demands for elevated data speeds, substantial diversity gain, and minimal channel utilisation loss in mobile telecommunication structures, MIMO antennas technologies has been extensively investigated [6], [7]. MIMO systems employ Utilisation of several transmitters at both the sender and reception to augment isolation, increase channel bandwidth, & alleviate multipath propagation effects [8], [9]. Recently, the integration of MIMO technology with UWB antenna systems has gained considerable research interest [10]. Modern wireless communication systems require antennas that offer low correlation coefficient, high diversity performance, and minimal co-channel interference, particularly in environments with obstacles and long-distance propagation [11]. In comparison with previously reported UWB MIMO antennas [10], improved axial ratio (AR) bandwidth is achieved in the recommended designing.

To enhance both impedance bandwidth and axial ratio performance, a T-shaped metallic parasitic strip (MPS) is introduced on the substrate between the dielectric resonator elements. Compact and wideband UWB MIMO Transceiver configurations have already been extensively documented in publications [12]–[18], where two-element MIMO antennas are typically arranged with 180° orientation to achieve high isolation. Reported designs generally exhibit insertion loss below −10 dB or −15 dB and E.C.C ≤ 0.5.

This study presents a unique lightweight rack-like structure two-element rectangular dielectric resonator

M.I.M.O antenna is recommended for ultra-wideband usage. The two dielectric resonator elements are positioned with a λ/2 separation, enabling monopole-like radiation behaviour, while the feedline acts as a filtering structure. A segment of landing planes via an integrated stub is implemented on the bottom surface of the layer to attain improved impedance matching & isolation. Additionally, a A T-form copper spurious strips is utilised to improve susceptibility range & axial ratio characteristics, enabling elliptically polarized radiation.

The key contributions of the suggested rack-formed dual-polarized MIMO antennas are summarized as follows:

- The antenna occupies a compact dimension of 39.6 × 29 mm² via a substrate height of 0.8 mm (ε_s = 4.4), while each dielectric resonator has dimensions of 14 × 9 × 5 mm³, offering high radiation efficiencies, least E.C.C, and ease of integration for UWB usage.
- A partially foundation plane using a balancing termination is implemented to enhance isolation, susceptibility matching, & impedance spectrum.
- A T-shaped parasitic-stripping is employed to achieving elliptical polarization, significantly improving axial ratio performance, where the axial ratio is reduced to ≤ 25.1 dB with the parasitic strip, compared to ≤ 41 dB without the strip (linearly polarized case).

II. Antenna Design and Configuration

In the present study, a novel 2-elements rectangular D.R.A based MIMO configuration is proposed, in which the radiator elements are separated by a latitude of λ/2 to attain superior segregation. A T-shaped metallic parasitic strip (MPS) is incorporated on the top layer of the substrates to augment its impedance range and attain a A.R of ≤ 24.9 dB. The overall antenna dimensions are 39.6 × 29 mm², fabricated on a substratting with dielectric const. of $\varepsilon_r = 4.4$ & a thickness of 0.8 mm. A partially grounded surface is established on the underside of the substrates, while the dielectric resonator structure and feedline are etched on the top side. Fig. 1 illustrates the geometry of the suggested M.I.M.O DRA. The antenna comprises two dielectric resonator radiating device fabricated using Rogers RT/duroid 6010 material with dielectric constant of $\varepsilon_{DR} = 10.2$. Each dielectric resonator has dimensions of 14 × 9 × 5 mm³ and is excited through a QWT-based microstrip feedline with dimensions of 4 × 1.9 mm² and 11 × 0.8 mm². As showing in Fig. 1(a) and Fig. 1(c), an inverting T-shaped parasitic-stripping is positioned on the upper surface of the substrating bet^{n} the dielectric resonators, while a partial grounded plane of dimension 37.6 × 9 mm² is inscribed on the underside of the material, whose overall dimensions are
37.6 × 29 × 0.8 mm³. Additionally, a rectangular stub of dimensions 9.2 × 3.5 mm² is introduced in the ground plane to further improve impedance matching and reduce mutual coupling (S_{21}).

The axial ratio performance of the antenna is controlling using the inverted T-formed parasitic strip, whose key geometrical parameters P_1, P_2, P_3, and P_4 are set to 16.8 mm, 7.9 mm, 2 mm, & 2.6 mm, respectively.

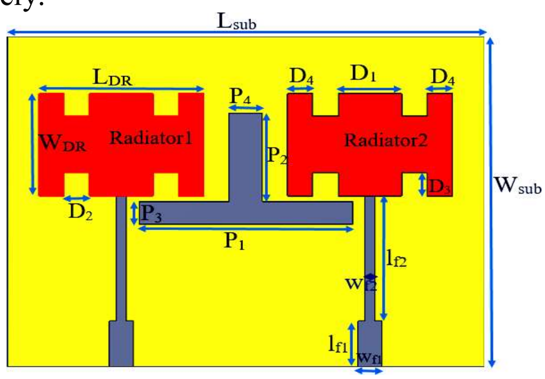

(a)

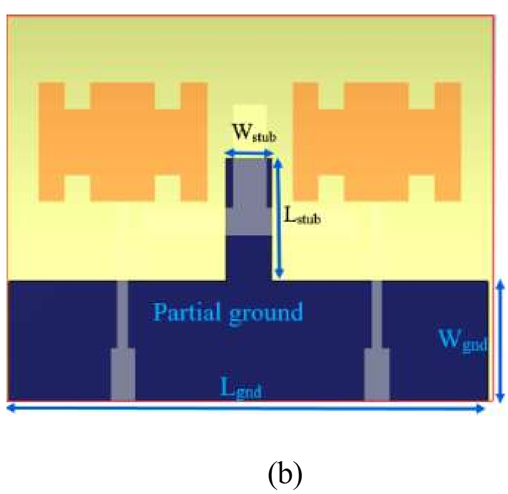

(b)

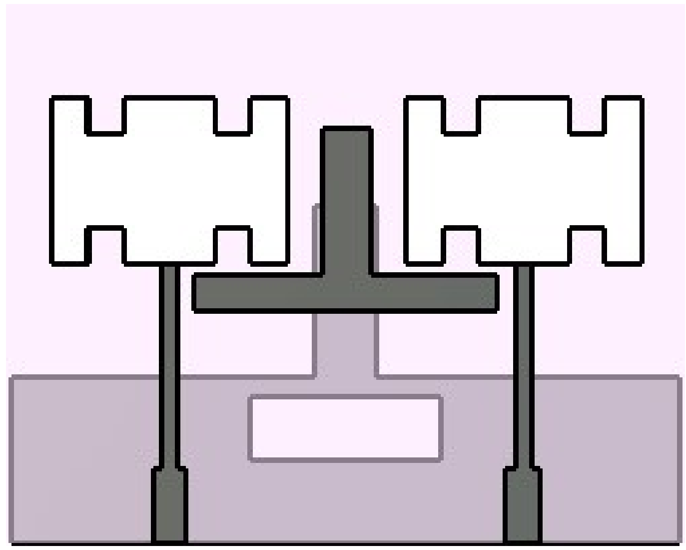

c)

Fig. 1 a-c Various perspectives of MIMO antennas

Table 1 Optimised parameters of MIMO antenna

Parameter	Values (mm)	Parameter	Values (mm)	Parameter	Values (mm)
L_{DR}	14	W_{stub}	3.5	D_3	2
W_{DR}	9	l_{f1}	4	D_4	2
L_{sub}	37.6	w_{f1}	1.9	P_1	16.8
W_{sub}	29	l_{f2}	11	P_2	7.9
L_{gnd}	37.6	w_{f2}	0.8	P_3	2
W_{gnd}	9	D_1	5	P_4	2.6
l_{stub}	9.2	D_2	2	H_{dr}	5

III. Antenna Stages

The stages of DRA are illustrated in Fig. 2 a-e. The simulated antennas undergoes five phases to attain the final design DRA 5. Step 1 involves a rectangular dielectric resonator (DR) with an altered grounding surface, achieving a peak attenuation ratio of 40 dB and consistent gain. In step 2, an appropriate stub is incorporated into the ground to enhance susceptibility compatibility & the transmittance efficiency (S21). Step 3 has altered the configuration of DR to enhance the propagation coefficients while marginally improving the range of impedance. In step 4, the electricity pathway of the transmitter is augmented through the incorporation of an inverted T-shaped degenerate component to attain the UWB band. In step 5, the suggested antenna is engineered to utilise a rectangle DGS slot incorporated into the ground plane to attain a significant peak gain of 9.4 dBi and an ultra-wideband bandwidth.

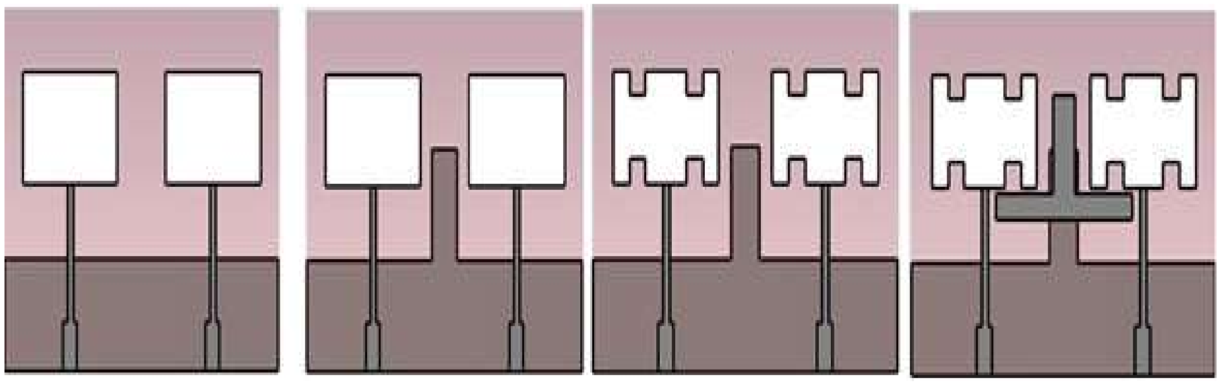

a) b) c) d)

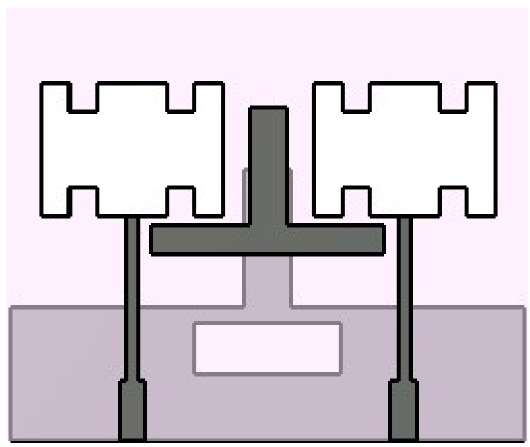

e)

Fig. 2 Performance analysis of antenna Stages a) DRA 1 b) DRA 2 c) DRA 3 d) DRA 4 e) DRA 5

IV. Result & Discussion

The antenna evolution process is illustrated through four design stages, denoted as DRA1–DRA4. In DRA1, a rectangular dielectric resonator is employed in conjunction with a partial ground planes. To enhance compatibility with impedance & inter-element coupling, a matching stub is introduced in the DRA2 configuration. In DRA3, the dielectric resonator is notching to form a rack-shaped geometry, enabling enhanced bandwidth characteristics. Finally, the DRA4 structure is further optimized by incorporating an inverting T-shaped parasitical band situated among the two radiating components to improve axial ratio performance and mutual-coupled reduction. As shown in Fig. 3(a)– (d), the progressive design modifications lead to significant performance enhancement. The suggested antenna attains a refraction ratio below −10 dB across the UWB frequency limit, with centre frequencies observed at 7.59 GHz, 7.50 GHz, 7.54 GHz, and 7.22 GHz for DRA1–DRA4, respectively. Additionally, the final configuration exhibits a substantial improvement in axial ratio bandwidth**, a** reduced coupling coefficient ranging from −15.6 dB to −55.4 dB**,** & a max.

realized gains of approximately 4.5 dB, confirming the efficacy of the suggested layout methodology.

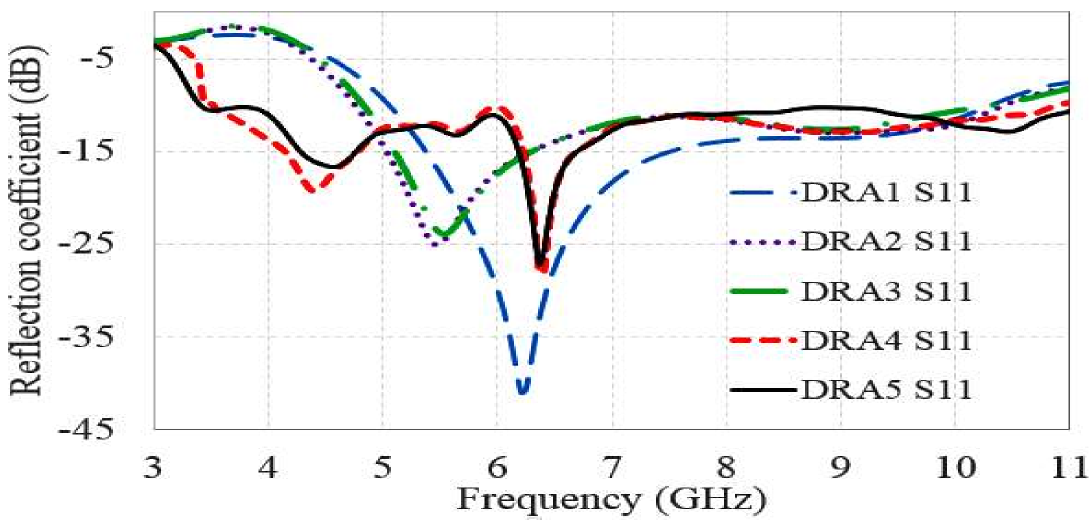

(a)

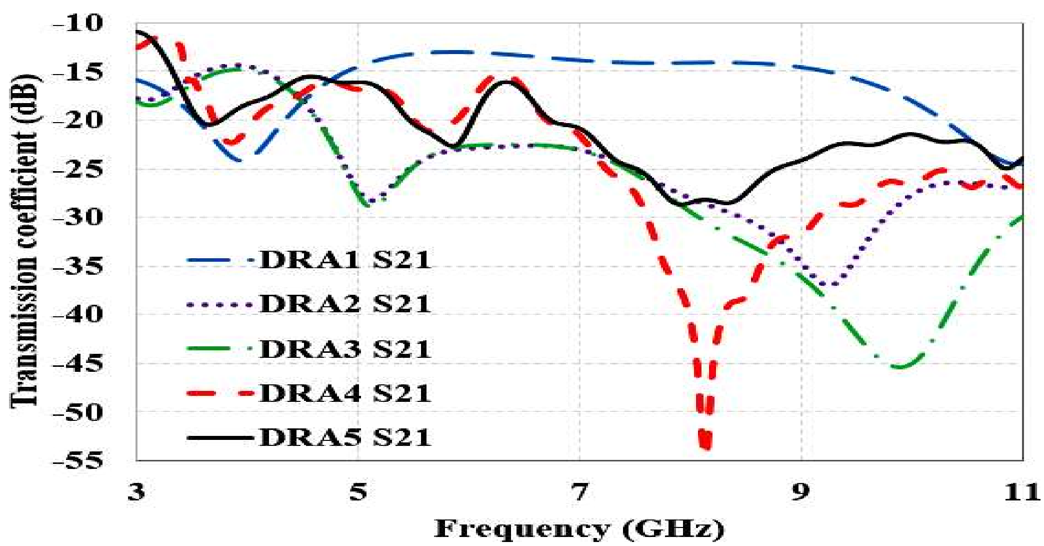

b)

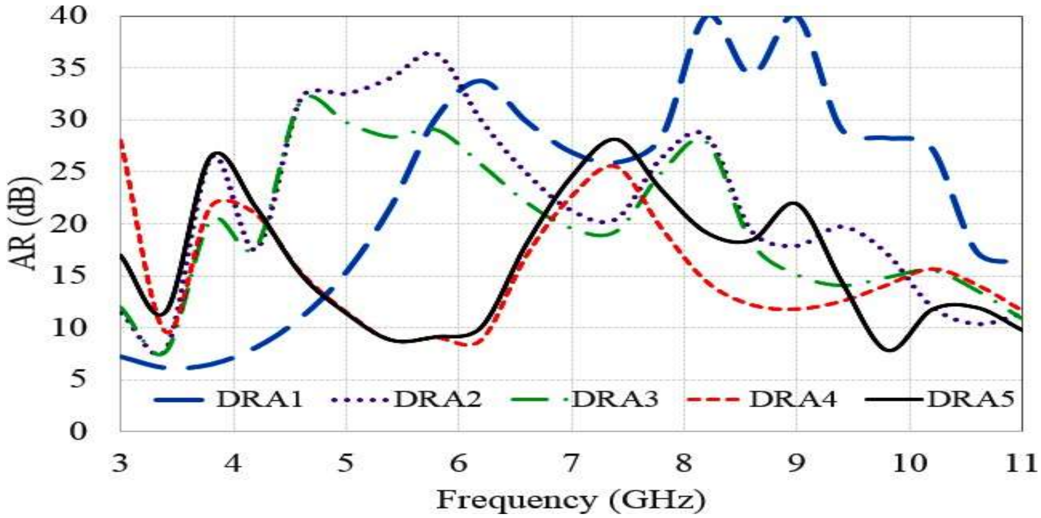

(c)

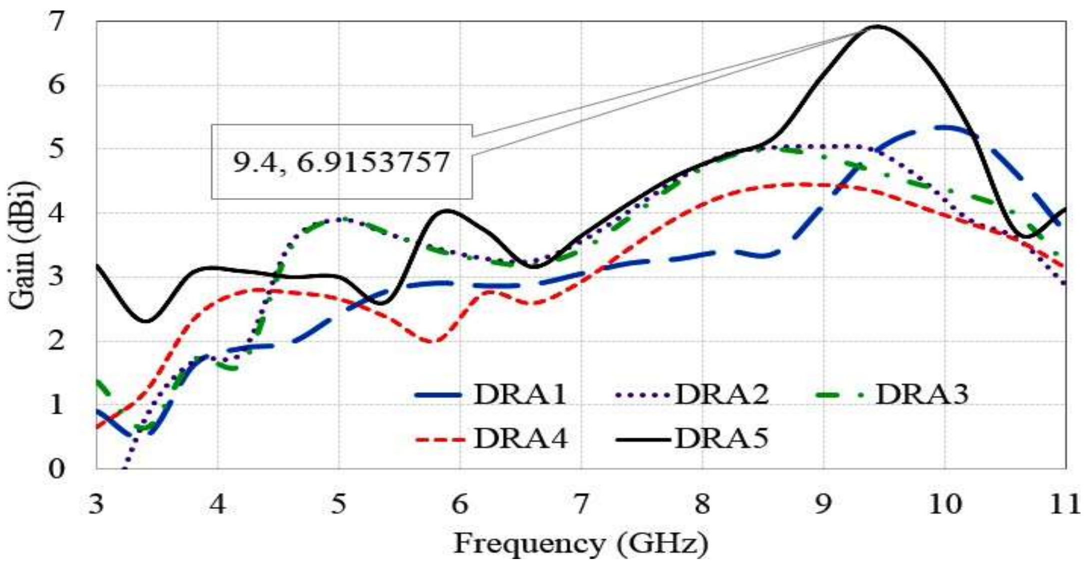

d)

Fig. 3 Bandwidth reaction regarding a) S_{11}, S_{22} parameters b) S_{21} parameter c) AR bandwidth d) Gain vs. frequency

Table 2 Step performance of all antennas

Step antenna	**S11, S22 10 dB**	**Impedance bandwidth %**	**S12, S21 (dB) Isolation**	**Gain range (dBi)**	**Axial ratio (dB)**

DRA1	5.09 to 10.1 GHz	66	12 to 26	0.5 to 5.4	6 to 41
DRA2	4.9 to 10.12 GHz	69.34	15 to 36	0.6 to 5.1	7.2 to 36.5
DRA3	4.8 to 10.28 GHz	72.67	16 to 46.1	0.8 to 5	7.1 to 33
DRA4	3.54 to 10.89 GHz	101.87	15.5 to 54.2	1.5 to 4.5	8.1 to 25.4
DRA5	3.32 to 11.1 GHz	106.2	16.8 to 29	1.8 to 9.4	8.1 to 27.3

All the evaluated performance the specifications are encapsulated in Table II. It has been noted that the proposed two-element M.I.M.O DRA5 configuration exhibits the best overall performance across the UWB frequency range, achieving an enhanced axial ratio bandwidth of ≤ 25.1 dB.

V. Results and Discussion of Fabricated Antenna

The suggested rack-shaped M.I.M.O dielectric resonator antenna (DRA) is simulated and fabricated on an FR4 substrate exhibiting a dielectric constant of $\varepsilon_r = 4.4$, a height of 0.8 mm, and a lossing-tangent of 0.0024. A photograph of the fabricated antenna prototype incorporating the metallic parasitic strip (MPS) is shown in Fig. 4(a). Figures 4(a) & 4(b) present the front and rear perspectives of the constructed antennas, respectively, highlighting the modified a portion ground level featuring an embedded corresponding stub inscribed on the material's inferior portion.

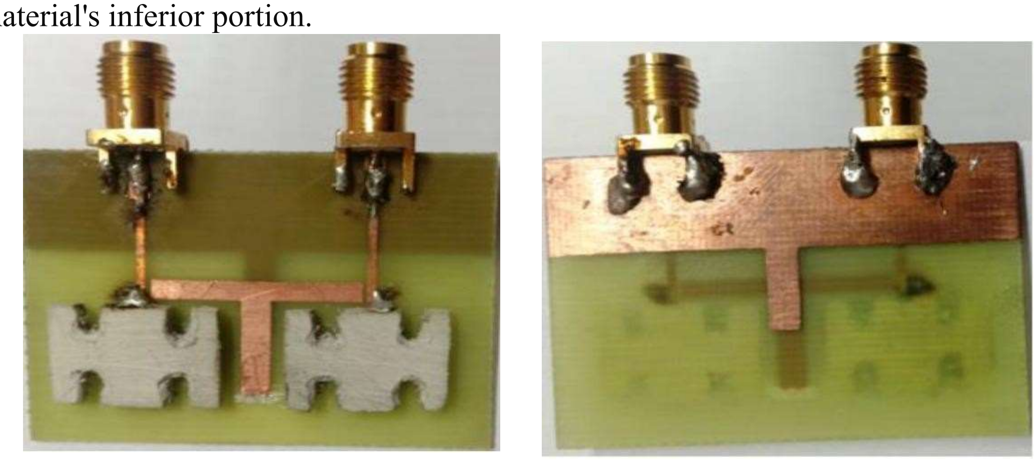

(a) (b)

Figure 4 Fabricated two radiator element MIMO antenna; a. Front view, b. Back view

The fabricated MIMO DRA prototype was experimentally characterized using a VNA (E5093A) to measure the S-parameters (S_{11}, S_{21}) and group delay. The The spectrum of radiation & realised gain of the suggested antennas were assessed in an Acoustic environment operating over the 2–18 GHz frequency range, employing a standard horn antennas via an efficiency of 12 dBi as the benchmark. All S-parameter measurements were conducted at IIT, Delhi, India.

Figures 5(a) and 5(b) present a Correlation of the generated & observed S-parameters, demonstrating the refraction ratio (S_{11}) and transmission coefficient (S_{21}), respectively. With the incorporation of the metallic parasitic strip (MPS), The suggested UWB MIMO DRA attains a 10-dB susceptibility spectrum of 101.87%. Figure 5(a) illustrates that the antennas have effective equal impedance throughout the whole UWB wavelength spectrum, ranging from 3.54 to 10.87 GHz. Moreover, Fig. 5(b) verifies that the suggested MIMO antenna delivers exceptional performance isolation, with the transmission coefficient maintained below −15.6 dB throughout the operating band.

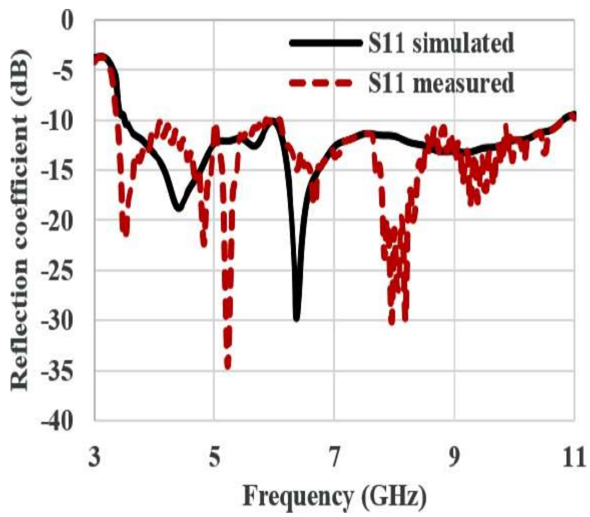

(a)

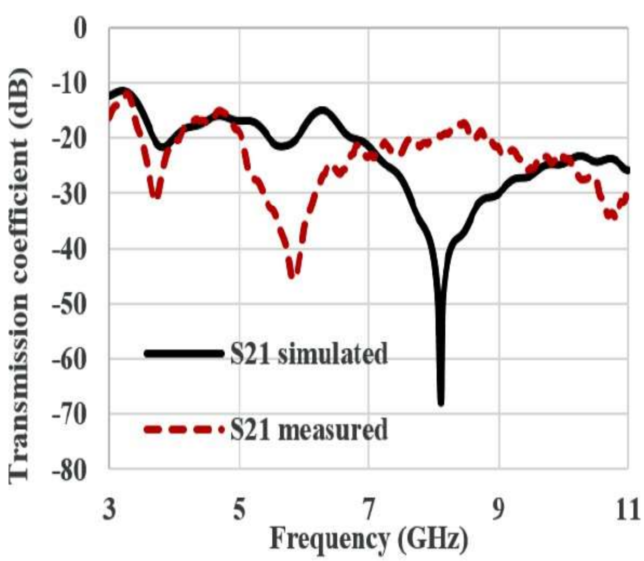

(b)

Figure 5: Simulating & measuring S- parameters; **a.** S11, **b.** S21

The efficacy of a MIMO antennas design is generally assessed by essential diversification measurements, including the overall coefficient of correlation, diversification gained (DG), complete actively reflected coefficients, and channel bandwidth loss. The simulated & measured ECC, calculated using the standard formulation given in (Equation X), is illustrated in Fig. 6. The E.C.C quantifies the level of correlation bet^{n} the multiple transmission channels at the broadcaster and reception via the propagation media. For the proposed U.W.B MIMO DRA, the E.C.C remains below 0.006 across the entire UWB frequency bandwidth, which is significantly less as compared to the commonly accepted threshold of 0.5, indicating excellent diversity performance. The diversity-gain (D.G) represented the enhancement in S.N.R at the receiver due to diversities techniques and is computed using the expression provided in (Equation Y). The proposed MIMO DRA exhibits a DG close to the idealised magnitude of 10 dB throughout the operated-bands. Figure 6 presents the frequency-dependent variation of both ECC and DG, confirming the superior diversity characteristics and effective MIMO performance of the suggested antenna system.

$$\mathrm{ECC}^{n} = \frac{|S^{*}_{11}\ S_{12}+S^{*}_{21}\ S_{22}|^2}{(1\text{-}|S_{11}|^2-|S_{21}|^2)\ (1\text{-}|S_{22}|^2-|S_{12}|^2)}$$

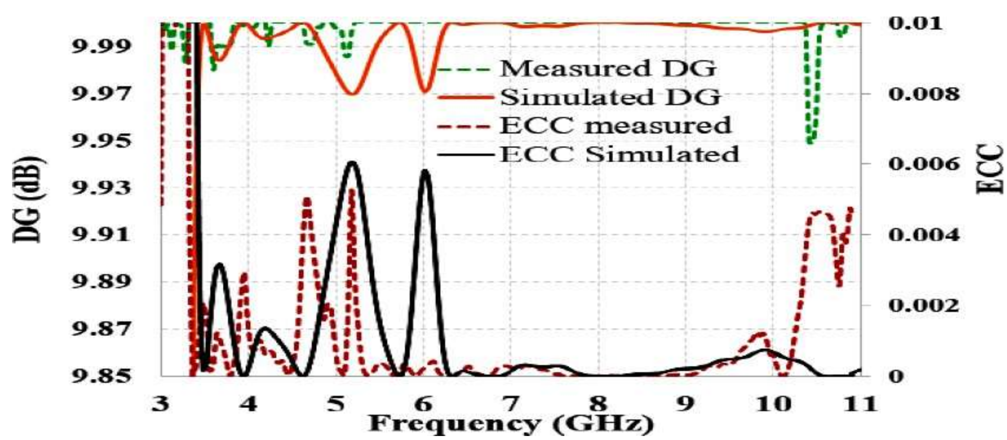

Figure 6 Simulating & calculated - measuring DG and E.C.C M.I.M.O antenna results

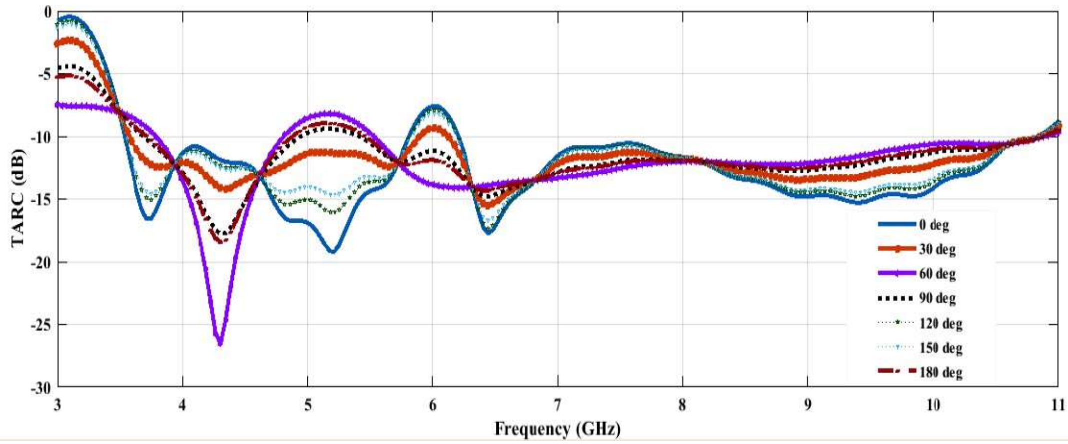

Figure 7 TARC diversity of MIMO antenna

Figure 7 illustrates the total active reflection coefficient (TARC), which is one of the essential MIMO diversity performance parameters. TARC characterizes the overall reflection behavior of a MIMO antenna system under simultaneous excitation of all ports and is evaluated using the two-port network representation. The impedance spectrum of the suggested antenna is determined from the 2-D TARC response, calculated using Equation .

$$\Gamma_a^{\text{Trans}} = \sqrt{\frac{(|S_{11}+S_{12}e^{j\theta}|^2+|S_{21}+S_{22}e^{j\theta}|^2)}{\sqrt{2}}}$$

where ΓaTrans= transmitted activation reflecting coefficient, θ is the incoming communication's processing phase.

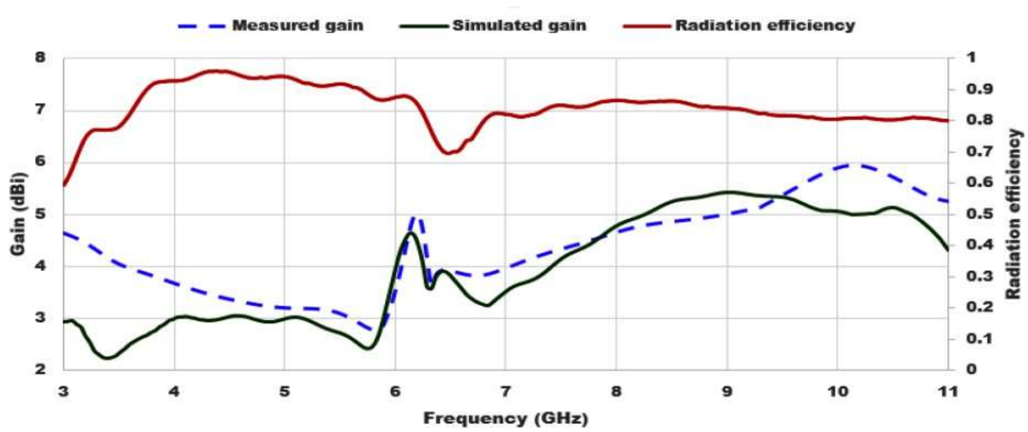

Figure 8: Gain and simulating Radiating efficiencies with frequencies

The radiating characteristics of the suggested two-element MIMO DRA are analyzed under standard excitation conditions. Assuming Port 1 is activated & Port 2 terminates using a 50

Ω matching demand, the electromagnetic spectrum distribution corresponding to Radiator 1 is

obtained. Conversely, by reversing the excitation i.e., exciting Port 2 while terminating Port 1 through a 50 Ω load the radiating features of Radiator 2 are evaluated. These excitation scenarios demonstrate the effective effectiveness of diversification in the suggested MIMO antennas design. The simulating and measuring two-dimensional radiation patterns and realized gain for both cases are presented in Fig. 8.

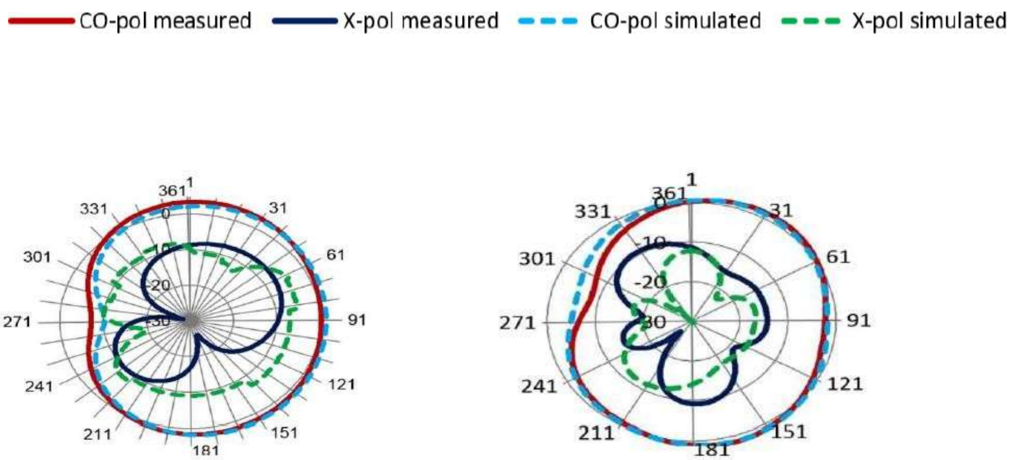

(a) (b)

Figure 9: Polarisation Radiating Distribution at; a. 4.3 GHz, b. 6.3 GHz

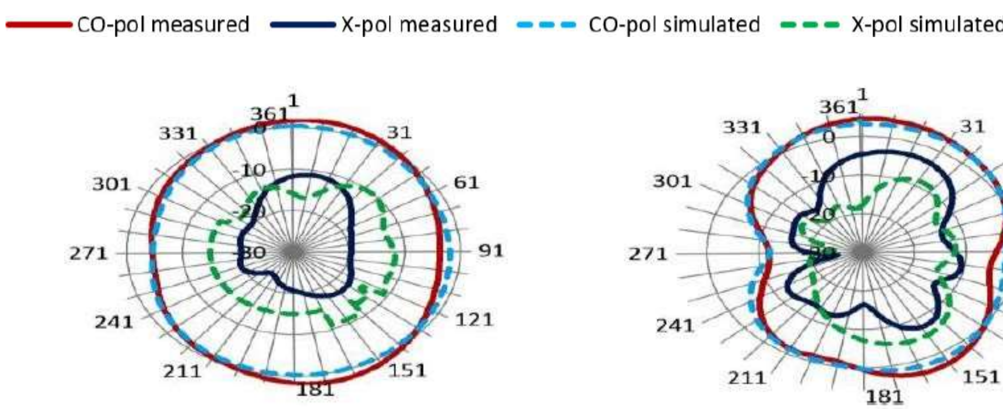

(c) (d)

Figure 10: Polarisation Radiating Distribution at; c. 8.4 GHz, d. 10.2 GHz

The radiating features of the proposed rack-shaping M.I.M.O dielectric resonator antennas

(DRA) are presented in Fig. 9. The co-polarized & cross-polarized radiating patterns are illustrated at operating frequencies of 4.3, 6.3, 8.4, and 10.2 GHz. At most of these frequencies, The cross-polarized values are significantly less than the respective co-polarized degrees levels, indicating efficient radiation performance and satisfactory polarization purity of the proposed antenna. A comprehensive examination of the planned rack-shaped MIMO DRA & several previously reporting UWB M.I.M.O antenna configurations is provided in Table III.

Without the parasitic strip (PS), the antenna exhibits a transmission coefficient of ≤ −21 dB & achieves a peak-gaining of 6.5 dBi; however, it fails to cover the entire UWB frequencies spectrum. An inversion T-formed parasitical band is inserted and affixed to the upper layer of the platform to mitigate this constraint. The inclusion of the parasitic strip effectively enhances the impedance bandwidth and axial ratio, enabling UWB operation, although a slightly degradation in gain is observing. The comparative performance of the antennas with & without the parasitic-strip is illustrated in Fig. 10.

Table 3 Comparative Analysis of U.W.B two element M.I.M.O antenna

Authors	Frequency band	S21, S12 (dB)	Gain	Size (mm3)	Group delay (ns)
M. Abedian	3.3 to 11.1 GHz	-15	5.3 dBi	29 × 29 × 5	N.R
Yanjie Wu	3.1–10.6 GHz	-18	N.R	22 × 35 × 0.8	N.R
Abhishek Sharma	3.24 to 6 GHz Wideband	-20	7.45 dBi	70 × 70 × 20.32	N.R
Suggested D.R.A antenna (With inverting T- shaped parasitic strip)	3.5 to 10.89 GHz	- 15.6	5.36 dBi	37.6 × 25 × 2.5	0.66 to -2.1

Table III presents a comparative analysis of the suggested cross-shaping metallic parasitic strip (MPS)-based M.I.M.O dielectric resonator antenna (DRA) with several widely documented MIMO DRA layout designed for U.W.B applications. The suggested crossed-shaped MPS antennas attains a transmitting effectiveness of 20 dB and a peak realised gain of 5.7 dBi. To enhance the impedance bandwidth and isolation performance, design techniques such as an inverting T-shaped MPS, a ground-plane stub, & a scissor-shaped defected ground structure (DGS) are incorporated.

Furthermore, Table IV compares the suggested cross-formed MPS-driven M.I.M.O D.R.A via existing MIMO MPA designs discussed in the previous work. The suggested antenna effectively covers the entire UWB frequency band from 3.3 to 10.8 GHz, while maintaining high isolating levels of ≥ 20 dB, demonstrating its suitability for UWB MIMO communication systems.

Table 4 Comparative Analysis of MIMO Patch Antennas with Suggested MIMO Dielectric Resonator Antenna

Reference	Frequency band (GHz)	S21 (dB)	Gain (dBi)	Substrate material	Substrate Size (mm^3)	ECC/ Diversity Gain (dB)
[13]	3.1-10.6	-18	-	FR4	25 × 35 × 0.8	0.005/-
[14]	3 – 11.4	-16	6.3	Taconic RF-35	40 × 35 × 0.8	0.01/9.95
[15]	3.1 – 14 (Four bands)	-15	2 - 6	εr = 2.65	30× 32 × 1.6	-/-
[16]	2.85 – 11.79	-20	2 to 5 dBi	FR4	L1 × L2 × 0.8	0.005/-
[17]	8 – 12	-20	2.67 -4.62	FR4	26× 18 × 1.6	0.01/-
[18]	2.5 – 2.7 3.4 – 3.6	-25	6.9 to 7.8 7.8 to 8.6	F4B, εr = 2.65	60× 100 × 0.8	0.46- 0.08/- 0.08- 0.01/-
[19]	3400 -3600 MHz , 5150–5925 MHz	-25	-	FR4	140× 70 × 1	0.05
Proposed MIMO DRA	3.3 to 10.8 GHz	-20	2.67 to 5.7 dBi	FR4	37.6 × 25 × 0.8	0.006/9.97

VI. Conclusion

The research work done to get the MIMO DRA for UWB operations of objective four is presented in this paper. Here, two antennas are designing, developed, fabricated, & tested. A novel UWB MIMO rack-shaped DRA exciting using a quarter-wave transforming (Q.W.T)- type feed line is suggested for UWB applications. The antenna achieves a wide impedance spectrum from 3.52 to 10.89 GHz, correspondence to a fractional spectrum of 101.87%, while maintaining good across element segregation greater than 15.6 dB. The proposed configuration comprises two rack-shaped dielectric radiator elements, an inverting T-shaping metallic parasitic-stripping, and a partial ground-planes with an integrated matching stub, which collectively enhance impedance matching and UWB performance.

Furthermore, the antennas exhibits good M.I.M.O diversity features, including a least ECC (ECC $\leq$ 0.0059), a large diversities gaining (D.G $\geq$ 9.94 dB), and a favourable transmission coefficient (≤ -15.6 dB) across the operated spectrum. The results validate the appropriateness of the suggested antennas for high-speed UWB MIMO communication networks.

References

[1] Docket, E.T. (2002). Docket 98–153, *FCC, Revision of part 15 of the commission's rules regarding ultra-wideband transmission systems*. Technical Report.

[2] Luk, K. M., & Leung, K. W. (2003). *Dielectric resonator antenna*. U. K.: Research Studies Press, UK.

[3] Yaduvanshi, R. S., & Parthasarathy, H. (2016). *Rectangular dielectric resonator antennas*. New Delhi, India: Springer.

[4] Mongia, R. K., & Bhartia, P. (1994). Dielectric resonator antennas—A review and general design relations for resonant frequency and bandwidth. *International Journal of Microwave and Millimeter-Wave Computer-Aided Engineering, 4*(3), 230–247.

[5] Pan, Y. M., & Zheng, S. Y. (2015). A low-profile stacked dielectric resonator antenna with high-gain and wide bandwidth. *IEEE Antennas and Wireless Propagation Letters, 15,* 68–71.

[6] Sharma, A., Sarkar, A., Biswas, A., & Akhtar, M. J. (2018). A-shaped wideband dielectric resonator antenna for wireless communication systems and its MIMO implementation. *International Journal of RF and Microwave Computer-Aided Engineering, 28*(8), e21402.

[7] Das, G., Sharma, A., & Gangwar, R. K. (2017). Dual feed MIMO cylindrical dielectric resonator antenna with high isolation. *Microwave and Optical Technology Letters, 59*(7), 1686–1692.

[8] Agarwal, A., & Kaur, A. (2017). A dual band stacked aperture coupled antenna array for WLAN applications. *Microwave and Optical Technology Letters, 59*(3), 648–654.

[9] Das, G., Sharma, A., & Gangwar, R. K. (2018). Triple-band hybrid antenna with integral isolation mechanism for MIMO applications. *Microwave and Optical Technology Letters, 60*(6), 1482–1491.

[10] Abedian, M., Rahim, S. K. A., Fumeaux, C., Danesh, S., Lo, Y. C., & Jamaluddin, M. H. (2017). Compact ultrawideband MIMO dielectric resonator antennas with WLAN band rejection. *IET Microwaves, Antennas and Propagation, 11*(11), 1524–1529.

[11] Das, G., Sharma, A., Gangwar, R. K., & Sharawi, M. S. (2018). Triple-port, two-mode based two element cylindrical dielectric resonator antenna for MIMO applications. *Microwave and Optical Technology Letters, 60*(6), 1566–1573.

[12] Ahmad Khan, A., Khan, R., Aqeel, S., Ur Rehman Kazim, J., Saleem, J., & Owais, M. K. (2017).

[13] Dual-band mimo rectangular dielectric resonator antenna with high port isolation for LTE applications. *Microwave and Optical Technology Letters, 59*(1), 44–49.

[14] Chae, S. H., Oh, S. K., & Park, S. O. (2007). Analysis of mutual coupling, correlations, and TARC in WiBro MIMO array antenna. *IEEE Antennas and Wireless Propagation Letters, 6,* 122–125.

[15] Sahu, N. K., Das, G., & Gangwar, R. K. (2018). Dual polarized triple-band dielectric resonator based hybrid MIMO antenna for WLAN/WiMAX applications. *Microwave and Optical Technology Letters, 60*(4), 1033–1041.

[16] Trivedi, K., & Pujara, D. (2017). Mutual coupling reduction in wideband tree shaped fractal dielectric resonator antenna array using defected ground structure for MIMO applications. *Microwave and Optical Technology Letters, 59*(11), 2735–2742.

[17] Nasir, J., Jamaluddin, M. H., Khalily, M., Kamarudin, M. R., Ullah, I., & Selvaraju, R. (2015). A reduced size dual port MIMO DRA with high isolation for 4G applications. *International Journal of RF and Microwave Computer-Aided Engineering, 25*(6), 495– 501.

[18] Wu, Y., Ding, K., Zhang, B., Li, J., Wu, D., & Wang, K. (2018). Design of a compact

UWB MIMO antenna without decoupling structure. *International Journal of Antennas and Propagation, 2018,* 1–8.

[19] Yadav, D., Abegaonkar, M. P., Koul, S. K., Tiwari, V. N., & Bhatnagar, D. (2018). Two element band-notched UWB MIMO antenna with high and uniform isolation. *Progress in Electromagnetics Research, 63,* 119–129.

[20] Lin, H., Song, Z., Wang, X., & Gao, H. (2017). An improved antenna group delay measurement method using a three-antenna extrapolation technique. *Radio engineering, 26*(3), 675–681.

[21] Yadav, S. K., Kaur, A., Khanna, R., et al. (2020). An ultra wideband "OM" shaped DRA with a defected ground structure and dual polarization properties for 4G/5G wireless communications. *International Journal of RF and Microwave Computer-Aided Engineering, 30*(8), e22327.